THE JOURNAL OF BIOLOGICAL CHEMISTRY VOL. 291, NO. 36, pp. 18675–18688, September 2, 2016


# The Effect of Fragmented Pathogenic α-Synuclein Seeds on Prion-like Propagation*[S]

Received for publication, April 25, 2016, and in revised form, June 22, 2016 Published, JBC Papers in Press, July 5, 2016, DOI 10.1074/jbc.M116.734707

**Airi Tarutani[‡§], Genjiro Suzuki[‡], Aki Shimozawa[‡§], Takashi Nonaka[‡], Haruhiko Akiyama[‡], Shin-ichi Hisanaga[§], and Masato Hasegawa[‡1]**

*From the [‡]Department of Dementia and Higher Brain Function, Tokyo Metropolitan Institute of Medical Science, Tokyo 156-8506, Japan and the [§]Department of Biological Science, Tokyo Metropolitan University, Tokyo 192-0397, Japan*

**Aggregates of abnormal proteins are widely observed in neuronal and glial cells of patients with various neurodegenerative diseases, and it has been proposed that prion-like behavior of these proteins can account for not only the onset but also the progression of these diseases. However, it is not yet clear which abnormal protein structures function most efficiently as seeds for prion-like propagation. In this study, we aimed to identify the most pathogenic species of α-synuclein (α-syn), the main component of the Lewy bodies and Lewy neurites that are observed in α-synucleinopathies. We prepared various forms of α-syn protein and examined their seeding properties *in vitro* in cells and in mouse experimental models. We also characterized these α-syn species by means of electron microscopy and thioflavin fluorescence assays and found that fragmented β sheet-rich fibrous structures of α-syn with a length of 50 nm or less are the most efficient promoters of accumulation of phosphorylated α-syn, which is the hallmark of α-synucleinopathies. These results indicate that fragmented amyloid-like aggregates of short α-syn fibrils are the key pathogenic seeds that trigger prion-like conversion.**

Amyloid-like intracellular abnormal protein deposits are the defining feature of many neurodegenerative diseases, and the distributions of these pathological proteins are closely correlated with disease symptoms and progression (1–3). Recently, it has been experimentally demonstrated that these abnormal proteins with amyloid-like cross-β structures have prion-like properties and propagate throughout the brain by converting normal proteins into abnormal forms. This prion-like mechanism may be the main pathogenetic pathway of major neurodegenerative disorders, including Alzheimer disease, Parkinson disease (PD),[2] and ALS.

α-Synucleinopathies, which include PD, dementia with Lewy bodies, and multiple system atrophy, are a subset of neurodegenerative diseases characterized by abnormal α-syn inclusions in neurons and/or glial cells (4). α-Syn is a 140-amino acid polypeptide whose physiological functions remain to be clarified, but it is localized in presynaptic terminals (5) and has roles in various synaptic functions (6–8). In α-synucleinopathies, aggregated, phosphorylated, and partially ubiquitinated α-syn is found as Lewy bodies in neuronal cell bodies and as Lewy neurites in dendrites in PD and dementia with Lewy bodies (9–12), whereas it is found as glial cytoplasmic inclusions in oligodendroglial cells in multiple system atrophy (13). Ultrastructurally, these abnormal α-syn aggregates exhibit filamentous or fibrous forms 5∼10 nm in width (14).

α-Syn is natively unfolded and highly water-soluble (15). However, under physiological conditions, purified recombinant human α-syn can polymerize into amyloid-like fibrils that morphologically and physicochemically resemble to those in brains of patients (16). Furthermore, preformed α-syn fibrils can work as templates to convert normal α-syn into amyloid-like fibrils *in vitro* and *in vivo* (17–20). Recapitulation of seed-dependent amyloid-like α-syn aggregation with phosphorylation and ubiquitination was demonstrated by introduction of preformed fibrils into cultured cells with transfection reagents (20). Similarly, seeded aggregation of α-syn was observed in primary cultured neurons into which extracellular preformed α-syn fibrils were incorporated by endocytosis, and Lewy body-like inclusions were formed (21, 22). Prion-like conversion of α-syn has also been demonstrated in animal models. Injection of preformed α-syn fibrils into brains of wild-type or transgenic mice overexpressing mutant human α-syn led to development of phosphorylated α-syn pathology several months later (17, 19, 23). In addition, injection of α-syn into different brain regions resulted in injection site-specific spreading of α-syn pathology, indicating that pathological α-syn spreads from cell to cell through neuronal networks (24). Furthermore, injection of sarkosyl-insoluble fraction containing pathological α-syn from synucleinopathies into wild-type or transgenic mice overexpressing mutant α-syn also caused α-syn pathology and neurodegeneration (19, 25, 26). Recent studies have suggested that

* This work was supported by Ministry of Education, Culture, Sports, Science, and Technology Grants-in-Aid for Scientific Research (KAKENHI) Grants JP26117005 (to M. H.) and JP26111730 (to T. N.), Japan Society for the Promotion of Science Grants-in-Aid for Scientific Research (KAKENHI) Grant JP23228004 (to M. H.), Ministry of Health, Labor, and Welfare of Japan Grant JP12946221 (to M. H.), a grant-in-aid for research on rare and intractable diseases, the Research Committee on Establishment of Novel Treatments for Amyotrophic Lateral Sclerosis, and Brain Mapping by Integrated Neurotechnologies for Disease Studies (Brain/MINDS) from the Japan Agency for Medical Research and Development (AMED) (to M. H.). The authors declare that they have no conflicts of interest with the contents of this article.

[S] This article contains supplemental Fig. S1.

[1] To whom correspondence should be addressed: Dept. of Dementia and Higher Brain Function, Tokyo Metropolitan Institute of Medical Science, Setagaya-ku, Tokyo 156-8506, Japan. Tel./Fax: 81-3-6834-2349; E-mail: hasegawa-ms@igakuken.or.jp.

[2] The abbreviations used are: PD, Parkinson disease; α-syn, α-synuclein; CBB, Coomassie Brilliant Blue; ThS, thioflavin S; MTT, 3-(4,5-dimethylthiazol-2-yl)-2,5-diphenyltetrazolium bromide.

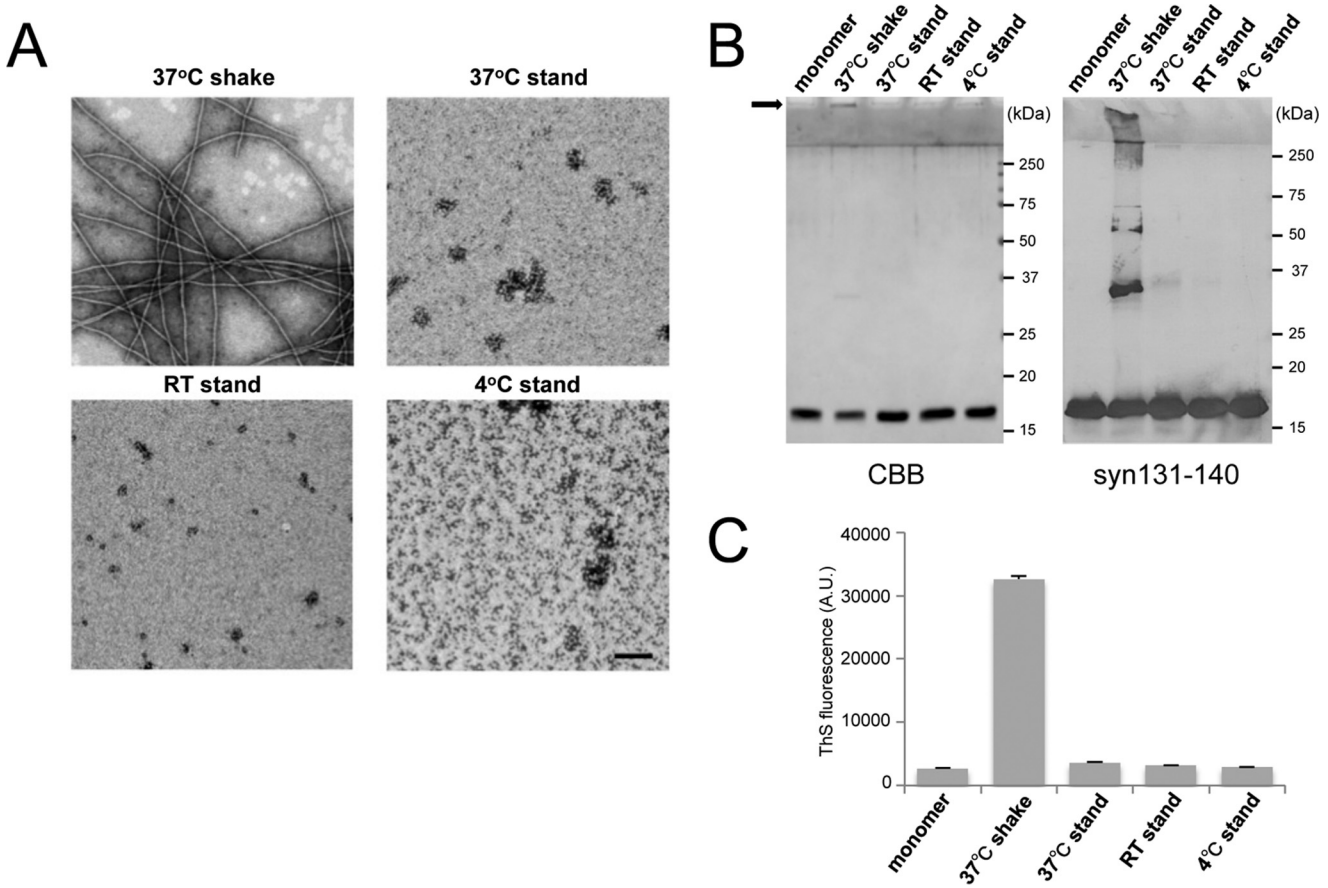


FIGURE 1. **Characterization of α-syn samples formed under various conditions.** *A*, electron microscopy of α-syn samples subjected to the following conditions: shaking at 37 °C, standing at 4 °C, room temperature (*RT*), and 37 °C for 7 days. Negatively stained fibrils and oligomer-like structures were observed. *Scale bar* = 200 nm. *B*, monomer α-syn and α-syn samples (0.5 μg of protein of each) were analyzed by CBB staining (*left panel*) and immunoblotting with anti-syn 131–140 antibody (*right panel*). The *arrow* indicates high molecular weight polymers in the gel top. *C*, ThS fluorescence of monomer α-syn and α-syn samples. The results are expressed as mean S.E. ($n = 3$). *A.U.*, arbitrary unit.

there are different kinds of α-syn strains with different biochemical properties (27), and injection of different α-syn fibril strains into rat brain caused strain-specific α-syn pathologies (28). These results clearly indicate that preformed α-syn fibrils have prion-like properties and that pathological α-syn can be transmitted between cells. Although preformed fibrils show prion-like activities, it has been suggested that granular or ring-like intermediates of fibrils, such as oligomers or prefibrils of various sizes, are neurotoxic, rather than the fibrils themselves (29–31). However, the oligomers are not well defined, and it remains uncertain whether they are actually intermediates in the pathway to fibrils. It is also unclear whether α-syn oligomers exist in brains of patients and are involved in disease pathogenesis *in vivo*.

As for the prion-like mechanism, it is also unclear what kinds of molecules (fibrils or oligomers, soluble or insoluble) are the most pathogenic, what sizes of these molecules are the most effective, and what mechanisms underlie the cell-to-cell spreading. Recent studies have indicated that structural differences in the pathological proteins may affect the efficiency of endocytosis or exocytosis and the seeding activity in cells as well as transport and toxicity (32–34).

In this study, we prepared various kinds of α-syn aggregates or intermediates under various conditions and tested their prion-like properties *in vitro*, in cells, and in mouse experimental models. We found that short amyloid-like fibrils with β sheet structures are the most effective triggers of prion-like conversion in all models. Our results indicate that α-syn fibrils less than 50 nm in size can act as prion-like assemblies.

## Results

*The Fibril Form of α-Syn Acts as Seed for Prion-like Conversion*—To investigate what kinds of α-syn species are most effective for prion-like conversion of normal α-syn into the abnormal form, we prepared several kinds of α-syn aggregates or intermediates under various conditions and examined their seeding ability. Purified recombinant human α-syn was incubated under the following conditions: standing at 4 °C, room temperature (20∼25 °C), and 37 °C or shaking at 37 °C. EM analysis after incubation for 7 days revealed that α-syn shaken at 37 °C formed fibrous structures (Fig. 1*A*). On the other hand, oligomer-like structures were observed in the samples at room temperature and 37 °C without shaking. Coomassie Brilliant Blue (CBB) staining of SDS-PAGE gels and immunoblotting of these α-syn samples showed that α-syn shaken at 37 °C contained SDS-stable dimers and high molecular weight polymers in addition to monomers (Fig. 1*B*). Thioflavin S (ThS) fluorescence intensity measurements of these samples indicated that

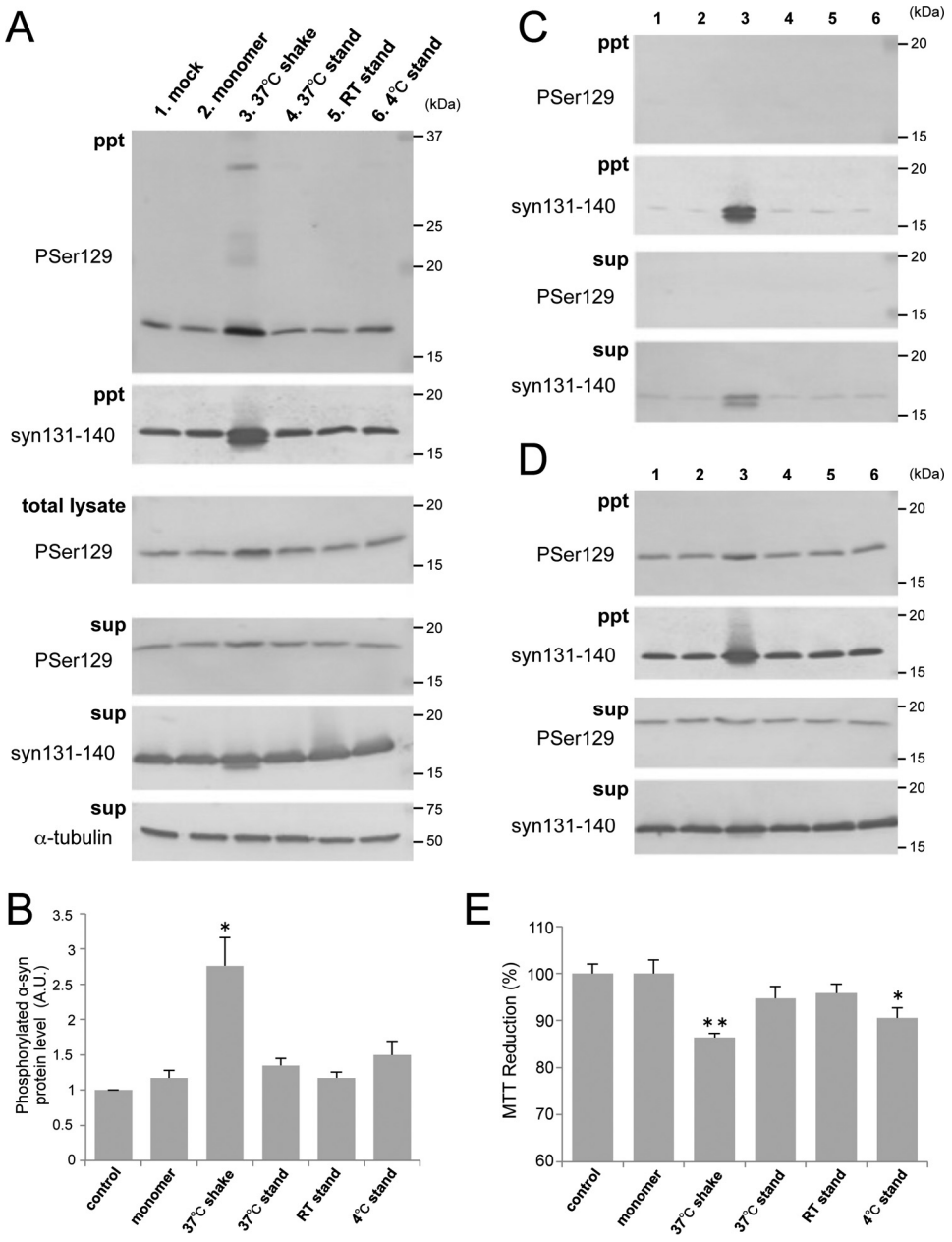


FIGURE 2. **α-syn fibrils cause seed-dependent aggregation in SH-SY5Y cells.** *A*, α-syn samples (5 μg) were introduced into SH-SY5Y cells overexpressing human α-syn in the presence of transfection reagent. Immunoblot analyses of sarkosyl-insoluble fractions (*ppt*), total cell lysates (*total lysate*), and sarkosyl-soluble fractions (*sup*) extracted from mock-transfected cells (*1*) and cells transfected with α-syn monomer (*2*), 37 °C shaking (*3*), 37 °C standing (*4*), room temperature (*RT*) standing (*5*), and 4 °C standing (*6*) are shown. Phosphorylated α-syn was detected with anti-phosphorylated α-syn Ser(P)-129 antibody. α-Syn was detected with anti-syn 131–140 antibody. *B*, quantification of immunoblot analyses shown in *A*. The results are expressed as mean ± S.E. ($n = 3$). *A.U.*, arbitrary unit. *C*, immunoblot analysis of sarkosyl-insoluble fractions and sarkosyl-soluble fractions extracted from cells without overexpression of human α-syn. *D*, immunoblot analysis of sarkosyl-insoluble fractions and sarkosyl-soluble fractions extracted from cells into which α-syn samples had been introduced in the absence of transfection reagent. *E*, MTT reduction of SH-SY5Y cells introduced with α-syn samples shown in *A*. The results are expressed as mean ± S.E. ($n = 6$). *, $p < 0.05$; **, $p < 0.01$; Student's *t* test against the value of monomer.

the fibril form of α-syn after shaking at 37 °C contained β sheet structures whereas the other oligomer-like structures did not (Fig. 1*C*). To examine the abilities of these α-syn forms to convert normal α-syn into the abnormal form, we introduced them as seeds in the presence of transfection reagent into SH-SH5Y cells ectopically expressing human α-syn and investigated the seeded aggregations of α-syn in these cells, as reported previously (20). Sarkosyl-insoluble phosphorylated α-syn similar to that in patients with α-synucleopathies (10) was detected in cells into which the fibril form of α-syn, but not monomeric α-syn or the other samples, had been introduced (Fig. 2, *A* and *B*). We also conducted experiments using cells not overexpressing human α-syn and cells into which α-syn samples had been introduced in the absence of transfection reagent and found similar propensities in both cases (Fig. 2, *C* and *D*). These results suggest that the fibril form of α-syn, but not the intermediates, is responsible for seeded aggregation. In the following SH-SY5Y cell-based experiments, we used a method corresponding to that used for Fig. 2*A* to introduce α-syn samples, as this appeared to be most effective for seeded aggregation of

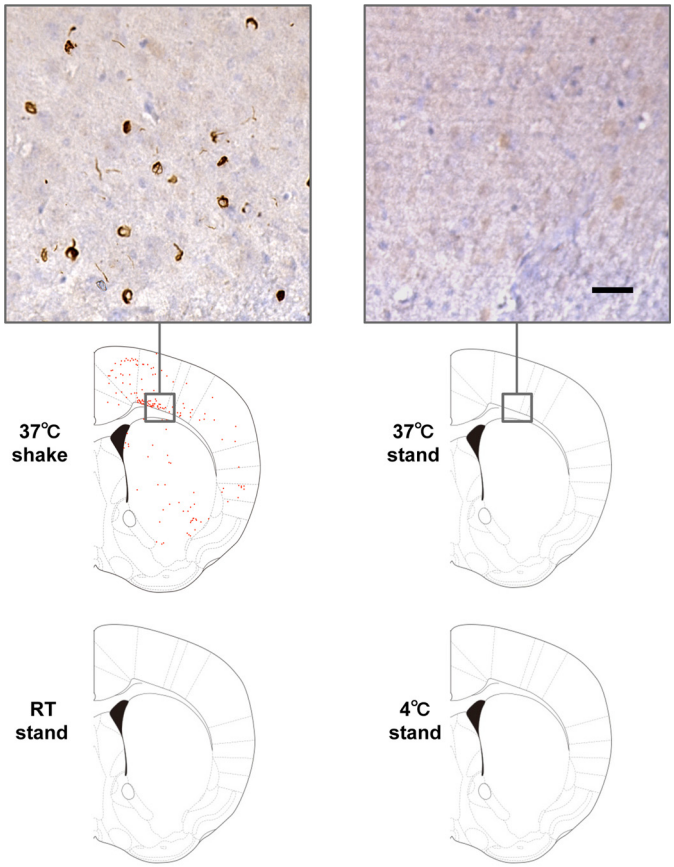


FIGURE 3. **α-Syn fibrils cause seed-dependent aggregation *in vivo*.** Distribution of phosphorylated α-syn pathology in mouse brain. WT mouse brain was injected with α-syn samples (10 μg) into striatum and observed 3 months later ($n = 7$ for 37 °C shaking, $n = 5$ for 37 °C standing, $n = 3$ for room temperature (*RT*) standing, $n = 2$ for 4 °C standing). Phosphorylated α-syn pathology was evaluated by immunohistochemistry with Ser(P)-129 antibody 1175. Typical images of brain injected with 37 °C shake (*left panel*) and 37 °C stand (*right panel*) are shown (*top panels*). Schematics of phosphorylated α-syn pathology at the level of 0.62 mm from the bregma are shown (*bottom panels*). *Red dots* indicate phosphorylated α-syn pathology. *Scale bar* = 25 μm.

α-syn. We also tested the cytotoxity of SH-SY5Y cells 2 days after introduction of α-syn samples by means of the widely used MTT assay (Fig. 2*E*). A significant reduction of MTT was detected in cells with intracellular accumulation of phosphorylated α-syn aggregates. To confirm good correspondence between the cellular model and mouse model, the same samples were injected into the striatum of C57BL/6J mice. As in the cellular model, accumulation of phosphorylated α-syn aggregates was observed 3 months after inoculation in mice inoculated with fibrils formed by shaking at 37 °C, whereas no such pathology was observed in mice inoculated with other samples (Fig. 3). These results suggest that only α-syn fibrils containing β sheet structures work as seeds for prion-like conversion of normal α-syn and cause aggregation of α-syn in both cultured cells and mouse brain.

*Seeding Activities of α-Syn Fractions Obtained by Centrifugation*—To further investigate what kinds of α-syn fibrils cause seed-dependent aggregation, α-syn fibrils after shaking at 37 °C were fractionated into supernatant and pellet by centrifugation, and the seed-dependent aggregation abilities of the fractions were examined. α-Syn fibrils formed by shaking at 37 °C for 7 days were sonicated by a tip-type sonicator or suspended by pipetting and then fractionated by centrifugation at 20,000 × *g* for 10 min. ThS fluorescence intensity measurements showed that the supernatant of the sonicated samples contained many amyloid-like fibrils, whereas suspended (unsonicated) samples contained less fibrils than the pellet (Fig. 4*A*). EM observation confirmed that fibrillar structures were present in the supernatants of both samples (Fig. 4*B*) and that more fragmented fibrils were found in the supernatant of the sonicated sample. To test the ability of these fractions to induce seed-dependent aggregation of α-syn, the fractions were introduced into SH-SY5Y cells, and the accumulation of sarkosyl-insoluble phosphorylated α-syn was examined (Fig. 4*C*). When the fractions from fibrils without sonication were introduced into cells, an increased level of phosphorylated α-syn was observed compared with cells treated with monomeric α-syn, and little difference was detected among the fractions (Fig. 4*D*). In contrast, a dramatic increase of phosphorylated α-syn was detected in the case of sonicated fibrils (total and supernatant), whereas only a small increase was observed after introduction of the pellet (Fig. 4*D*), strongly suggesting that short, fragmented fibrils formed by sonication, which were ThS-positive, efficiently acted as seeds. Next, to confirm whether the supernatant fraction also causes abnormal accumulation of α-syn *in vivo*, it was injected into mouse brain, and pathological changes of α-syn were evaluated 3 months later by immunohistochemistry with a phospho-α-syn antibody (Fig. 4*E*). The Supernatant of sonicated α-syn fibrils also induced accumulation of phosphorylated α-syn in mouse brain. These results indicated that fragmented α-syn fibrils in the centrifugal supernatant are the major cause of seed-dependent aggregation of α-syn in both cultured cells and mouse brain and are the most effective seeds among the forms of α-syn examined.

*Seeding Activity of α-Syn Fibrils Fragmented by Sonication*—To further investigate the effect of sonication and to examine the relationship between fibril size and seeding activity, we prepared different sizes of fibrils by sonication and tested their seeding activity. α-Syn fibrils formed by shaking at 37 °C were sonicated for various time periods, and the resulted fibrils were observed with an EM (Fig. 5*A*). Without sonication, many elongated fibrils were seen, but as the time of sonication was increased, the α-syn fibrils became shorter and more fragmented. Semiquantitative analysis of fibril lengths showed that short fibrils of less than 50 nm in length constituted ~80% of fibrils that had been sonicated for 180 s (Fig. 5*B*). However, the fluorescence intensity of ThS did not change, indicating that β sheet content and ThS accessibility were unaffected by the fragmentation (Fig. 5*C*). Next we examined whether fragmentation affected the seeding ability and prion-like properties *in vitro* and *in vivo*. First, to test whether these fragmented fibrils can act as seeds for prion-like conversion of the normal α-syn monomer into fibrils *in vitro*, we incubated monomeric α-syn with a small amount of these fibrils as seeds and measured the kinetics of ThS fluorescence (Fig. 5*D*). Fragmented fibrils accelerated the polymerization of α-syn monomers, whereas fibrils without sonication showed little effect. Moreover, the acceleration increased in direct proportion to sonication time, suggesting that shorter fibrils are more effective for seed-dependent aggregation. We also examined the seeding effects of diluted soni-

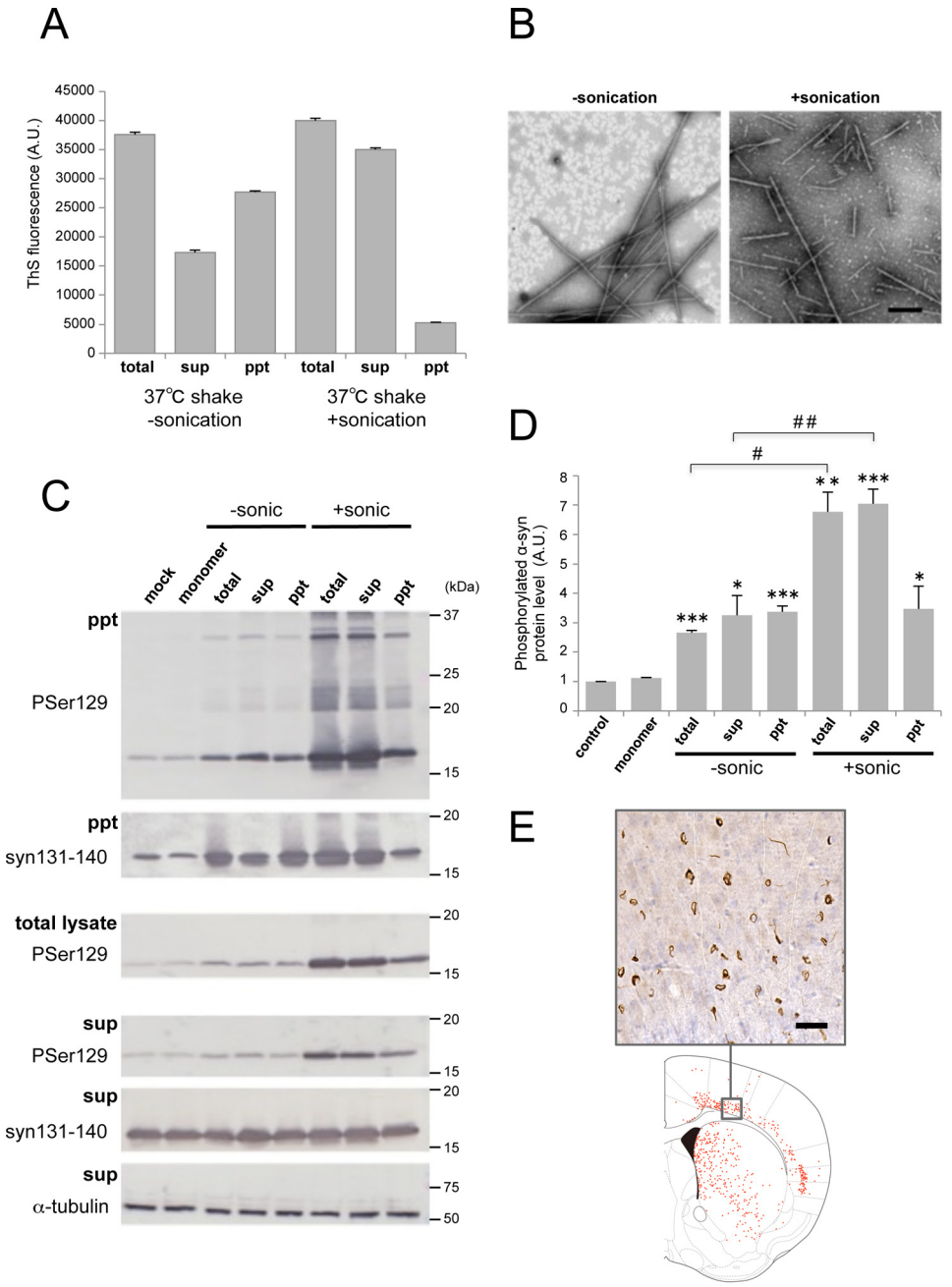


FIGURE 4. **Seeding activities of α-syn fractions obtained by centrifugation.** *A*, thioflavin S fluorescence of α-syn fibrils shaken (*shake*) at 37 °C for 7 days without or with sonication. Total α-syn (*total*) was fractionated into supernatant (*sup*) and pellet (*ppt*) by centrifugation. The results are expressed as mean ± S.E. ($n = 3$). *B*, electron microscopy of α-syn fibrils in supernatant after centrifugation without sonication (*left panel*) or with sonication (*right panel*). *Scale bar* = 200 nm. *C*, α-syn samples (2.5 μl) were introduced into SH-SY5Y cells overexpressing human α-syn. Immunoblot analysis of sarkosyl-insoluble fractions (*ppt*), total cell lysates (*total*), and sarkosyl-soluble fractions (*sup*) extracted from mock-transfected cells and cells transfected with α-syn monomer, α-syn samples without sonication (−*sonic*), total α-syn, supernatant, and pellet and α-syn samples with sonication (+*sonic*), total α-syn, supernatant, and pellet are shown. Phosphorylated α-syn was detected with anti-phosphorylated α-syn Ser(P)-129 antibody. α-Syn was detected with anti-syn 131–140 antibody. *D*, quantification of the immunoblot analysis shown in *C*. The results are expressed as mean ± S.E. ($n = 3$). *, $p < 0.05$; **, $p < 0.01$; ***, $p < 0.001$; Student's *t* test against the value of monomer. #, $p < 0.01$; ##, $p < 0.001$; Student's *t* test (without sonication *versus* with sonication). *E*, distribution of phosphorylated α-syn pathology in mouse brain. WT mouse brain was injected with supernatant after centrifugation of sonicated α-syn fibrils (10 μg) into striatum and observed 3 months later ($n = 2$). Phosphorylated α-syn pathology was evaluated by immunohistochemistry with Ser(P)-129 antibody. A typical image of brain (*top panel*) and a schematic of phosphorylated α-syn pathology (*bottom panel*) at the level of 0.62 mm from the bregma are shown. *Red dots* indicate phosphorylated α-syn pathology. *Scale bar* = 25 μm. *A.U.*, arbitrary unit.

cated fibrils (180 s) and compared them with that of unsonicated fibrils (Fig. 5*E*). The kinetics of ThT seeded with unsonicated fibrils were similar to those after seeding with 1/40- or 1/60-diluted sonicated fibrils, indicating that the seeding activity was dependent on the number of fibrils ends. Next, these fragmented fibrils were introduced into SH-SY5Y cells, and the accumulation of sarkosyl-insoluble phosphorylated α-syn was examined (Fig. 6*A*). As with the seeding assay *in vitro*, accumulation of sarkosyl-insoluble α-syn increased significantly in direct proportion to the sonication time of the fibrils

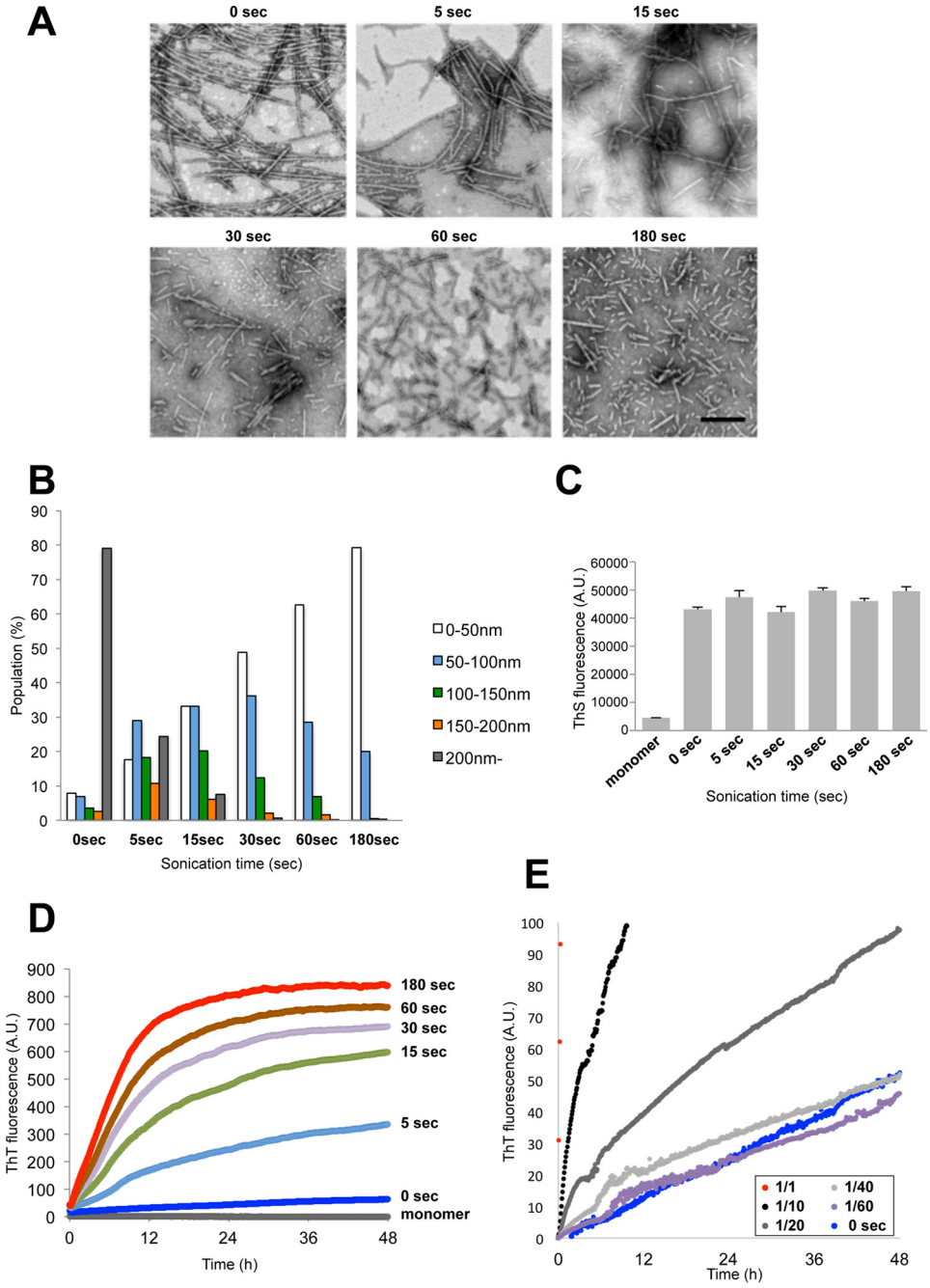


FIGURE 5. ***In vitro* seeding activity of α-syn fragmented by sonication.** *A*, electron microscopy of α-syn fibrils after sonication for 0, 5, 15, 30, 60, and 180 s. *Scale bar* = 200 nm. *B*, distribution of fibril length of sonicated α-syn fibrils. *C*, thioflavin S fluorescence of monomer α-syn and sonicated α-syn fibrils. The results are expressed as mean ± S.E. ($n = 3$). *D*, ThT fluorescence of monomer α-syn after addition of sonicated α-syn fibrils. *E*, ThT fluorescence of monomer α-syn after addition of α-syn fibrils without sonication (*0 s*) or various dilution series (*1/1* to *1/60*) of sonicated α-syn fibrils (*180 s*). *A.U.*, arbitrary unit.

(Fig. 6*B*). Regarding cytotoxity, there was a significant correlation between increased amounts of phosphorylated α-syn and MTT reduction (Fig. 6*C*). To examine the effect of fragmentation on incorporation into cells, the fibrils were labeled with Alexa 567 and introduced into cells, and imaging of the live cells was performed (supplemental Fig. S1). Incorporation of fragmented fibrils into cells was frequently observed, whereas unsonicated fibrils were clumped and hardly incorporated.

Furthermore, we examined whether accumulation of phosphorylated α-syn was also increased in mice inoculated with α-syn fibrils. These sonicated α-syn fibrils were injected into mouse brain, and pathological changes were examined 3 months later by means of immunohistochemistry of phosphorylated α-syn. Compared with inoculation of untreated α-syn fibrils (Fig. 1*D*), fragmented α-syn fibrils (such as fibrils sonicated for 180 s) caused more extensive seed-dependent aggregation and wider-ranging propagation of phosphorylated α-syn as we had observed in cultured cells (Fig. 7, *A* and *B*). Also, thioflavin T-positive aggregates were observed in fibril-injected mouse brains (Fig. 7*C*). Phosphorylated α-syn deposits resembling Lewy bodies and Lewy neurites were observed in the striatum, amygdala, substantia nigra, somatosensory cortex, cingu-

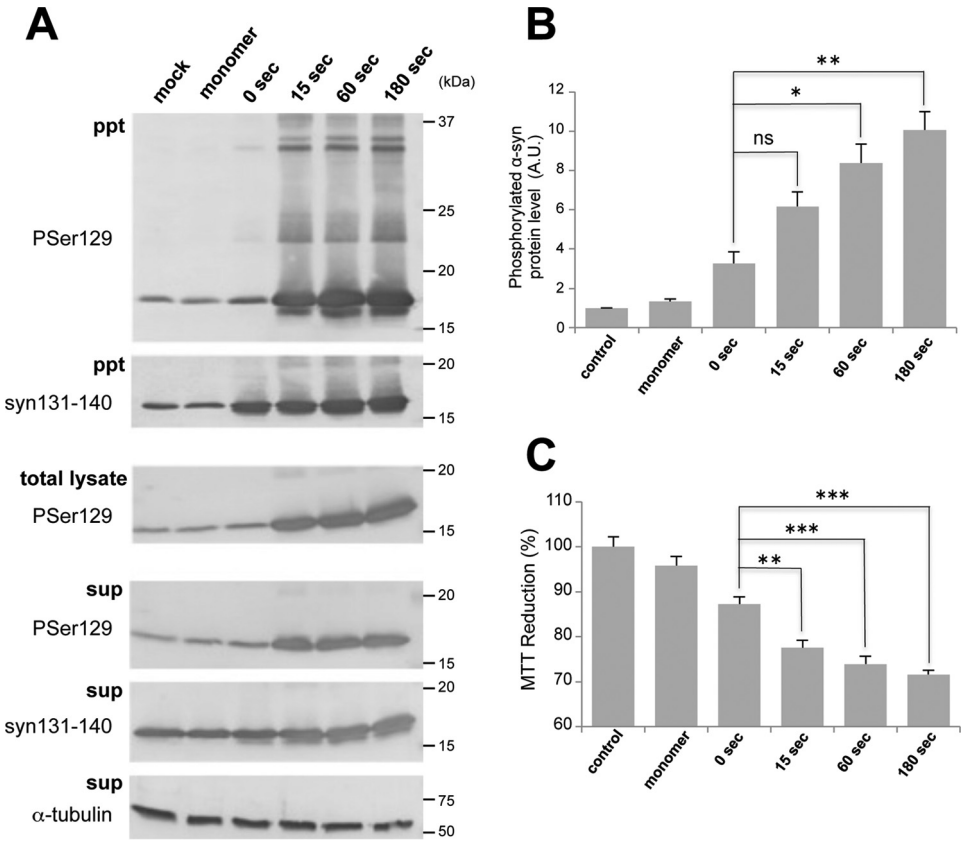


FIGURE 6. **Seeding activity in cultured cells of α-syn fragmented by sonication.** *A*, α-syn samples (5 μg) were introduced into SH-SY5Y cells overexpressing human α-syn. Immunoblot analysis of sarkosyl-insoluble fractions (*ppt*), total cell lysates (*total lysate*), and sarkosyl-soluble fractions (*sup*) extracted from mock-transfected cells and cells transfected with α-syn monomer and α-syn fibrils after sonication for 0, 15, 60, and 180 s. Phosphorylated α-syn was detected with anti-phosphorylated α-syn Ser(P)-129 antibody. α-Syn was detected with anti-syn 131–140 antibody. *B*, quantification of the immunoblot analysis shown in *A*. The results are expressed as mean ± S.E. ($n = 3$). *A.U.*, arbitrary unit. *C*, MTT reduction of SH-SY5Y cells introduced with α-syn samples shown in *A*. The results are expressed as mean ± S.E. ($n = 6$). *ns*, not significant; *, $p < 0.05$; **, $p < 0.01$; ***, $p < 0.001$; Student's *t* test against the value of 0 s.

late cortex, and corpus callosum, as reported previously (24) (Fig. 7*D*). Thus, sonication of α-syn fibrils had a significant effect on the accumulation of phosphorylated α-syn in mouse brain. Regarding the propagation patterns of α-syn accumulation, there was little difference between samples sonicated for 60 and 180 s, whereas phospho-syn pathology induced by the sample sonicated for 15 s was less extensive than that induced by the sample sonicated for 180 s. These results showed that more extensively fragmented α-syn fibrils also have a higher ability to cause seed-dependent aggregation of α-syn in mouse brain. It is possible that more extensive fragmentation of α-syn fibrils allows them to be incorporated into cells more efficiently, resulting in increased seeding activity for prion-like propagation because of greater acceleration of α-syn polymerization.

*Isolation of α-Syn That Causes Seed-dependent Aggregation by Gel Filtration Chromatography*—To characterize the fragmented α-syn fibrils and their effects on seed-dependent aggregation of α-syn, sonicated α-syn samples were fractionated by gel filtration chromatography, and the prion-like properties of the fractions were examined. α-Syn fibrils with or without sonication and monomer were fractionated based on molecular weight by means of gel filtration chromatography (Fig. 8*A*). One broad single peak with a retention time of 4 min (fraction 5) was detected for monomeric α-syn. A single peak with a retention time of 2 min (fraction 2) at the position of the void volume and a small peak at 5 min were detected when α-syn fibrils sonicated for 180 s were fractionated, whereas only a small peak at 5 min was detected when unsonicated α-syn fibrils were fractionated (full-length fibrils seemed to be retained in the precolumn filter). EM analyses of these fractions showed that short fibrils were recovered in fraction 2, whereas no such fibrils were detected in fraction 5 (Fig. 8*B*). Furthermore, fragmented α-syn fibrils sonicated for various times were fractionated, and samples of fractions 2 and 5 were analyzed by CBB staining of SDS-PAGE gels and ThS fluorescence assays (Fig. 8*C*). A large amount of α-syn protein was recovered in fraction 5 from the monomeric α-syn sample, but little α-syn was detected from α-syn fibrils. ThS fluorescence intensity in fraction 5 from all samples was not increased, indicating that monomeric α-syn protein was eluted in fraction 5. The amount of α-syn protein in fraction 2 increased in proportion to the sonication time and corresponded to the increase of ThS fluorescence intensity. These results indicated that short fibrils with a β sheet-rich structure were present in fraction 2. No peak was detected from the sample of α-syn fibrils without sonication, suggesting that long fibrils were not eluted from the column under the conditions used. Next, samples from fraction 2 were introduced into SH-SY5Y cells, and seed-dependent aggregation of α-syn was examined. Introduction of fraction 2 eluted from α-syn fibrils sonicated for 180 s resulted in the

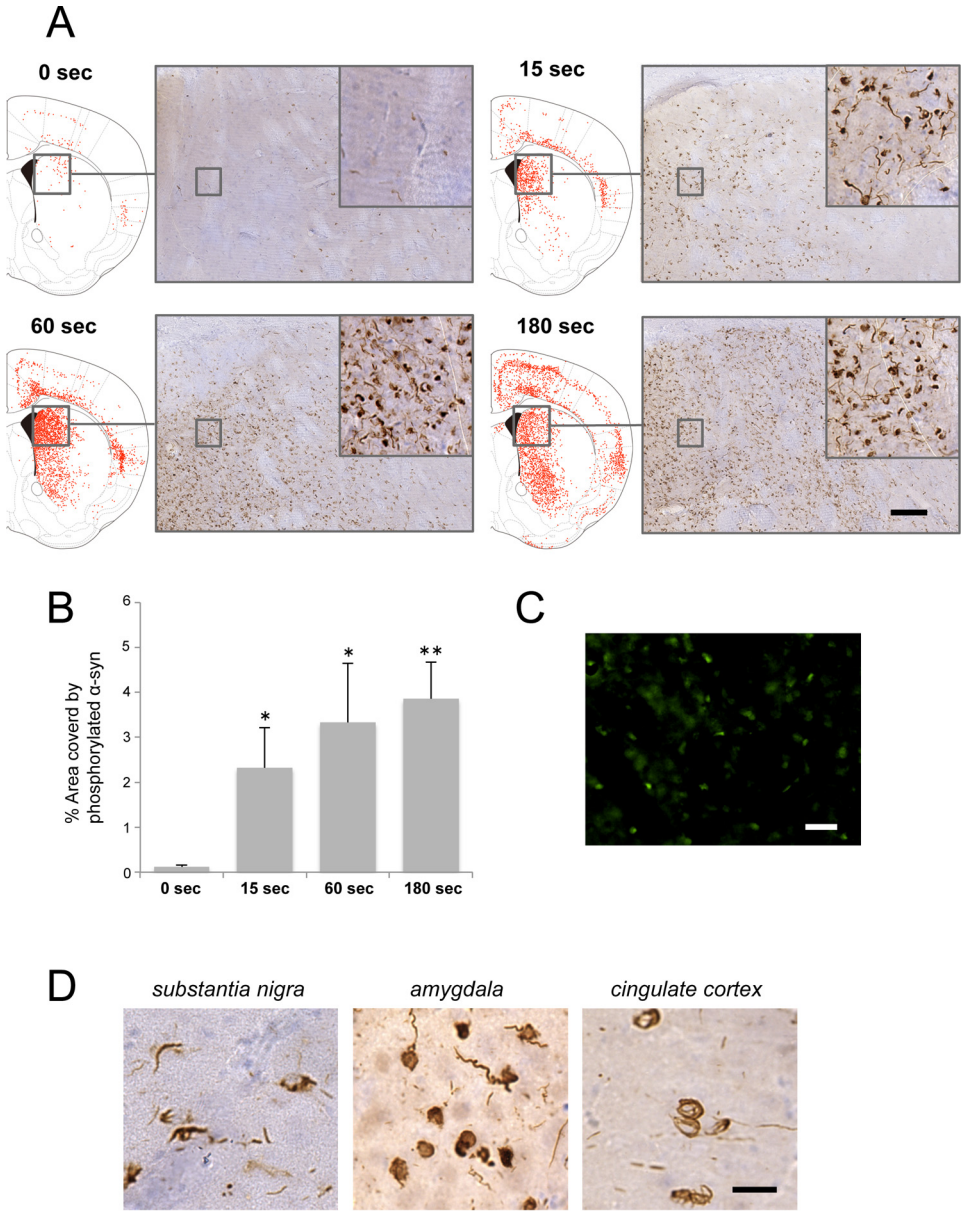


FIGURE 7. ***In vivo* seeding activity of α-syn fragmented by sonication.** *A*, distribution of phosphorylated α-syn pathology in brains of mice observed 3 months after injection of α-syn samples (10 μg) into striatum (*Str*). Phosphorylated α-syn pathology was evaluated by immunohistochemistry with Ser(P)-129 antibody. Typical images (*right panels*) and schematics of phosphorylated α-syn pathology (*left panels next to images*) at the level of 0.62 mm from the bregma of brain injected with α-syn fibrils sonicated for 0 s ($n = 7$, *top left panel*), 15 s ($n = 3$, *top right panel*), 60 s ($n = 3$, *bottom left panel*), and 180 s ($n = 3$, *bottom right panel*) are shown. *Red dots* indicate phosphorylated α-syn pathology. *Scale bar* = 100 μm. *B*, quantification of α-syn pathology in mice injected with α-syn fibrils into striatum. The results are expressed as mean ± S.E. ($n = 3$). *, $p < 0.05$; **, $p < 0.01$; Student's *t* test against the value of 0 s. *C*, ThT staining in striatum of mice injected with α-syn fibrils sonicated for 180 s into striatum. *Scale bar* = 25 μm. *D*, widespread phosphorylated α-syn pathology in mice injected with α-syn fibrils sonicated for 180 s into striatum. *Scale bar* = 20 μm.

highest accumulation of sarkosyl-insoluble phosphorylated α-syn (Fig. 8, *D* and *E*). In addition, accumulation of phosphorylated α-syn was highly correlated with the amount of α-syn fibrils recovered in fraction 2. These results showed that short α-syn fibrils in the void volume fraction had a potent ability to cause seed-dependent aggregation of α-syn.

*Isolation of the sarkosyl-insoluble Fraction from α-Syn-injected Mice*—To examine whether fibril forms of α-syn, such as those observed in the brains of α-synucleinopathies, exist in mouse brain injected with α-syn fibrils, we performed immunoelectron microscopy and isolation of pathological α-syn from mouse brain injected with mouse or human α-syn fibrils. Immuno-EM observation 23 months after inoculation revealed that numerous phosphorylated α-syn (Ser(P)-129)-positive fibrous structures had accumulated around the nuclei in neuronal cells of wild-type mouse brain injected with mouse α-syn fibrils (Fig. 9*A*). Next, the sarkosyl-insoluble fraction was prepared from mouse brain injected with monomeric human α-syn or human α-syn fibrils 18 months after inoculation. Immuno-EM observation demonstrated that fibrous α-syn structures were present only in the sarkosyl-insoluble fraction from α-syn fibril-injected mouse brain (Fig. 9*B*). The fibrils were ~10 nm in diameter, which is similar to those found in brains of α-synucleinopathy patients (14). These fibrous struc-

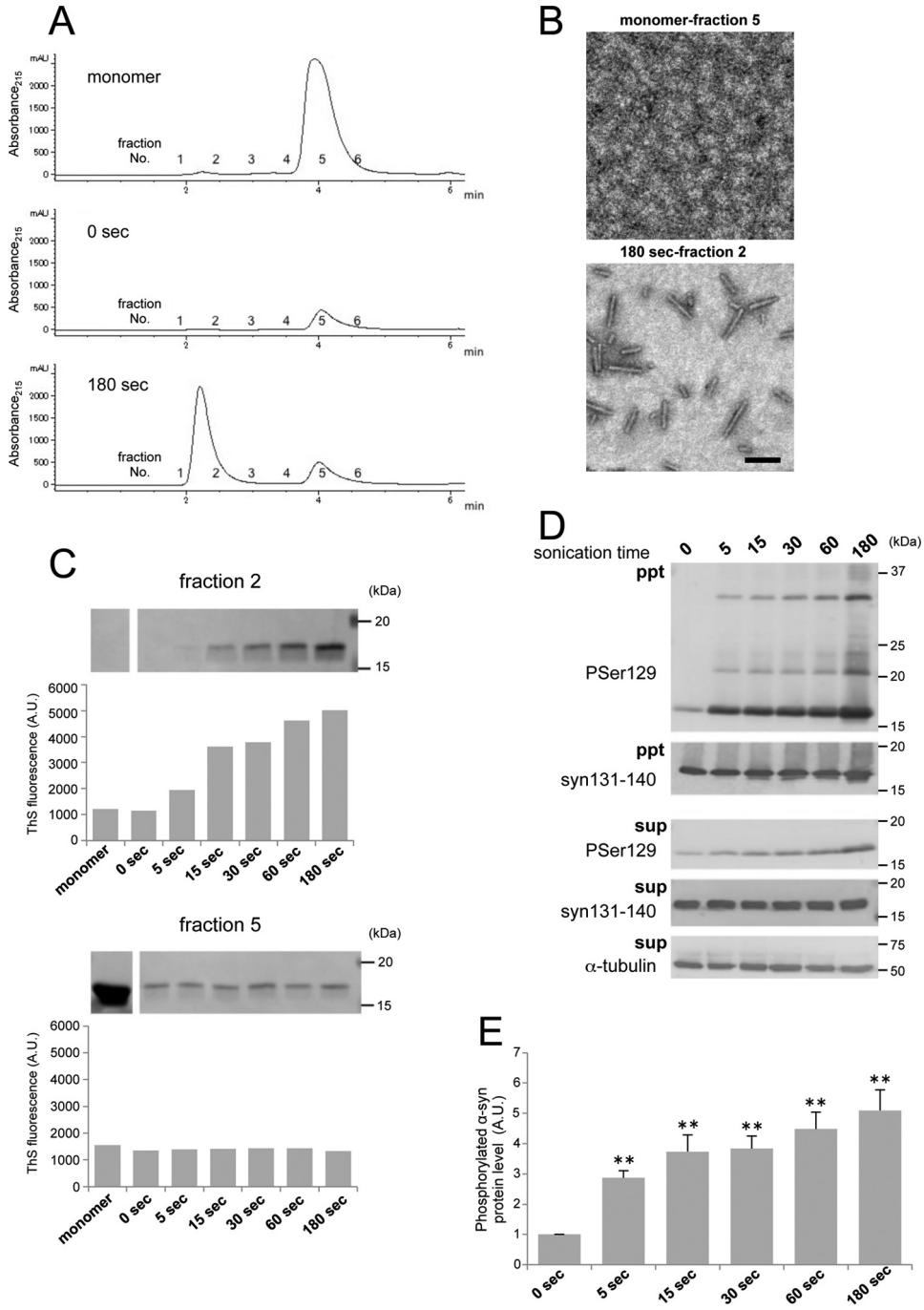


FIGURE 8. **Isolation of α-syn with seed-dependent aggregation ability by means of gel filtration chromatography.** *A*, isolation of monomeric α-syn and α-syn fibrils. Monomer α-syn and α-syn fibrils with or without sonication were fractioned by gel filtration chromatography. Fractions were collected every 0.5 min. *B*, electron microscopy of fraction 5 (*top panel*) isolated by gel filtration chromatography from monomer α-syn and fraction 2 (*bottom panel*) isolated from α-syn fibrils after sonication for 180 s. *Scale bar* = 200 nm. *C*, SDS-PAGE and ThS fluorescence of fraction 2 (*top panel*) and fraction 5 (*bottom panel*) isolated by gel filtration chromatography from monomer α-syn and α-syn fibrils after sonication for 0, 5, 15, 30, 60, and 180 s. *D*, fraction 2 (10 μl) was introduced into SH-SY5Y cells overexpressing human α-syn. Immunoblot analysis of sarkosyl-insoluble fractions (*ppt*) and sarkosyl-soluble fractions (*sup*) extracted from cells transfected with fraction 2 isolated by gel filtration chromatography from α-syn fibrils sonicated for 0, 5, 15, 30, 60, and 180 s. Phosphorylated α-syn was detected with anti-phosphorylated α-syn Ser(P)-129 antibody. α-Syn was detected with anti-syn 131–140 antibody. *E*, quantification of the immunoblot analysis shown in *D*. The results are expressed as mean ± S.E. ($n = 3$). **, $p < 0.01$; Student's *t* test against the value of 0 s. *A.U.*, arbitrary unit.

tures were positively stained with antibodies to syn131–140 and phosphorylated α-syn and also an antibody specific for mouse α-syn, indicating that endogenous mouse α-syn is accumulated as fibrous forms. Immunoblot analysis indicated that accumulated endogenous mouse α-syn was phosphorylated in fibril-injected mice but not in monomer-injected mice or fibrils prepared *in vitro* (Fig. 9*C*). To investigate whether these sarkosyl-insoluble fractions extracted from injected mice can induce seed-dependent aggregation of α-syn, they were introduced into SH-SY5Y cells, and the accumulation of sarkosyl-insoluble phosphorylated α-syn was examined (Fig. 9*D*). The introduction of sarkosyl-insoluble fractions extracted from α-syn fibril-

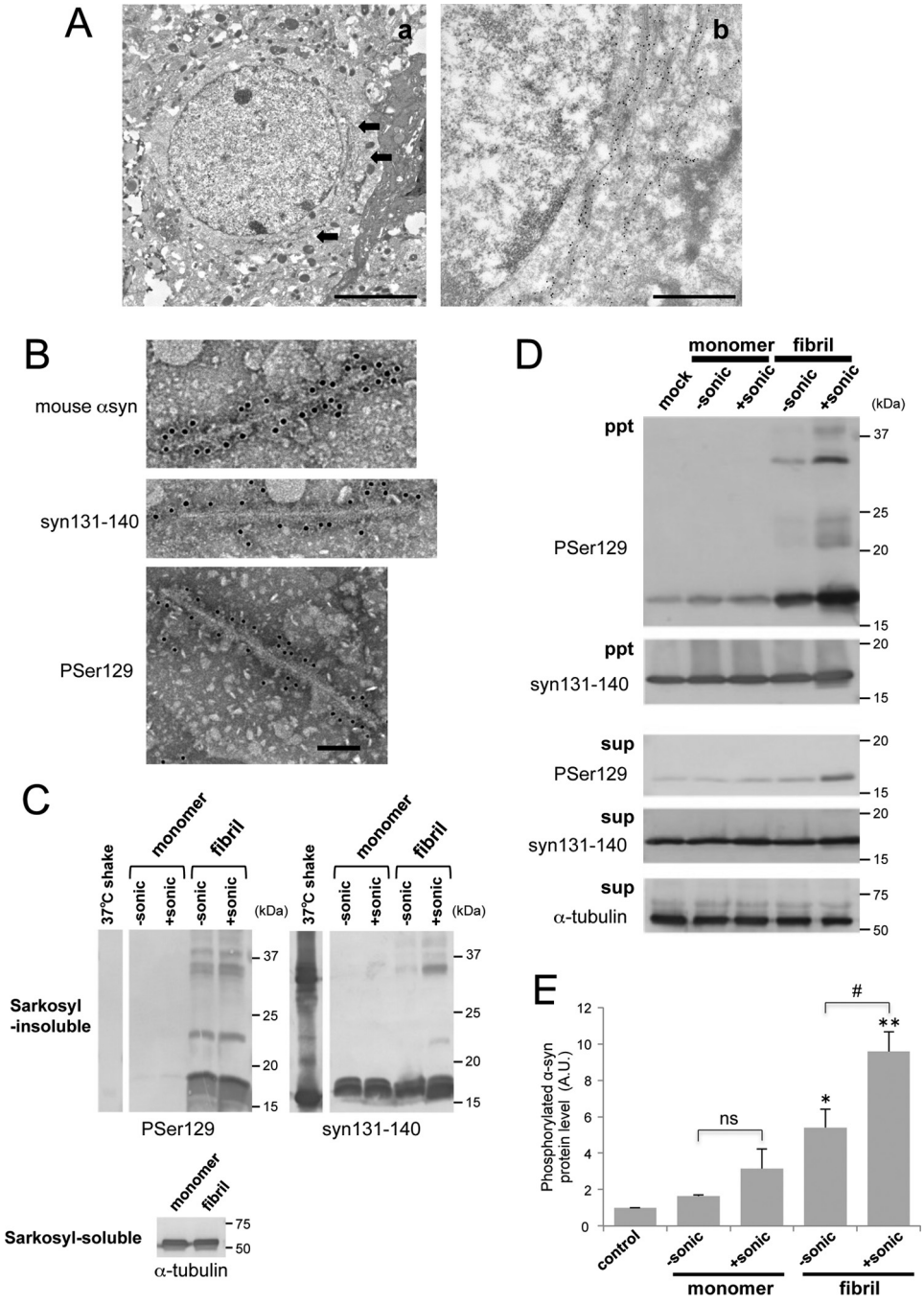


FIGURE 9. **Seeding activities of filaments extracted from α-syn fibril-injected mice.** *A*, immunoelectron microscopy of anti-phosphorylated α-syn-positive fibrous structures (*arrows*) in the brain of a mouse injected with α-syn fibrils, detected with gold particles. *Scale bars* = 5 μm (*a*) and 1 μm (*b*). *B*, immunoelectron microscopy of sarkosyl-insoluble fractions extracted from mice injected with sonicated α-syn fibrils. Anti-mouse α-syn-positive (*top panel*), anti-α-syn-positive (*syn 131–140*, *center panel*), and anti-phosphorylated α-syn-positive (*Ser(P)-129*, *bottom panel*) fibrous structures labeled with gold particles were observed. *Scale bar* = 100 nm. *C*, sarkosyl-insoluble fractions prepared from injected mice without (−) or with (+) sonication were analyzed by immunoblot with anti-phosphorylated α-syn Ser(P)-129 antibody and anti-syn 131–140 antibody. *D*, immunoblot analysis of sarkosyl-insoluble fractions (*ppt*) and sarkosyl-soluble fractions (*sup*) extracted from SH-SY5Y cells overexpressing human α-syn transfected with mouse brain extracts injected with α-syn monomers or fibrils without (−) or with (+) sonication. Phosphorylated α-syn was detected with anti-phosphorylated α-syn Ser(P)-129 antibody. α-Syn was detected with anti-syn 131–140 antibody. *E*, quantification of the immunoblot analysis shown in *D*. The results are expressed as mean ± S.E. ($n$ = 3). *, $p < 0.05$; **, $p < 0.01$; Student's *t* test against the value of monomer (−*sonic*). *ns*, not significant; #, $p < 0.05$; Student's *t* test (without sonication *versus* with sonication). *A.U.*, arbitrary unit.

injected mice resulted in accumulation of phosphorylated α-syn whereas the same fraction from monomer-injected mice did not. Furthermore, sonication of the introduced sarkosyl-insoluble fractions increased the accumulation of phosphorylated α-syn (Fig. 9*E*). These results demonstrate that fibrous structures similar to those observed in α-synucleinopathy patient brains were formed in α-syn fibril-injected mouse brain and that fibrils containing sarkosyl-insoluble fractions extracted from injected mice functioned as seeds for seed-dependent aggregation of α-syn.

## Discussion

Many *in vitro* and *in vivo* experimental models have demonstrated that the intracellular abnormal proteins characteristic of major neurodegenerative diseases, such as α-syn in PD, tau in Alzheimer disease, and TDP-43 in ALS/frontotemporal lobar degeneration have prion-like properties and that the intracellular conversion of normal proteins into abnormal forms and cell-to-cell spreading of the abnormal forms can occur. To understand the relationships between the phenomena in experimental models and those in brains of patients, we investigated the prion-like properties (transmissibility) of various α-syn species *in vitro*, in cells, and in animal models, as reported previously (19, 20). Our findings indicate that short α-syn fibrils with lengths of less than 50 nm are the most effective molecular triggers of the formation and spreading of abnormal α-syn by acting as seeds for prion-like conversion in cultured cells and mouse brains.

In our *in vitro* experiment, conversion of normal soluble α-syn into amyloid-like fibrils was accelerated by addition of small amounts of preformed α-syn fibrils, and the acceleration was increased in proportion to the sonication time of the fibrils (Fig. 5*D*), suggesting that fragmentation of the fibrils is important for the prion-like conversion. Indeed, the similarity of kinetics of α-syn fibril formation seeded with unsonicated fibrils and 1/40- or 1/60-diluted sonicated fibrils implies that the seeding activity was dependent on the number of fibril ends and that the number of fibrils was increased 40 to 60 times after sonication for 180 s (Fig. 5*E*). This seems consistent with the observed lengths of fibrils (Fig. 5*B*). In cultured cells, introduction of fragmented α-syn fibrils also promoted seed-dependent aggregation (Fig. 6*A*). This finding is consistent with a previous report showing that short fibrils induce seeded aggregation of endogenous α-syn in cultured cells without overexpression (35). We also found that increased cytotoxicity was correlated with increased accumulation of intracellular phosphorylated α-syn aggregates (Fig. 6*C*), but the observed cytotoxicities were comparatively low. This low propensity for cytotoxicity may be consistent with the extremely long silent period from the accumulation of α-syn aggregates until neuronal loss in patient brains. In mice, fragmented α-syn fibrils in which more than 80% of fragments were less than 50 nm in size were the most efficient for prion-like propagation (Fig. 7*A*). Although exogenously injected α-syn fibrils were degraded within a week (19), fragmented fibrils may continue to act on endogenous mouse α-syn until they are digested, generating widespread pathology. Therefore, control of propagation may require a focus on newly generated seeds.

Lewy bodies and Lewy neurites observed in patients are composed of filamentous α-syn 200–600 nm in length and 5–10 nm in width (14). Similarly, immuno-EM of α-syn fibril-injected wild-type mouse brain in this study revealed numerous comparatively long fibrous structures with approximately 10 nm width around nuclei (Fig. 9*A*). The accumulations of fibrous structures were also confirmed by immuno-EM of sarkosyl-insoluble fractions of mouse brains with antibodies specific for mouse α-syn and phosphorylated α-syn (Fig. 9*B*). These results indicated that recombinant α-syn fibrils acted as a pathogenic factor to convert endogenous mouse α-syn into amyloid-like fibrils. Furthermore, sonication of sarkosyl-insoluble fractions containing these fibrils resulted in enhancement of the seeding activity in cultured cells (Fig. 9*D*), raising the possibility that the breaking of once-elongated fibrils into short fragments *in vivo* enhances the prion-like activities of seeds, promoting cell-to-cell spreading. This is consistent with a report that fragmented amyloid-like fibrils have distinct properties of long fibrils (33), indicating that fragmentation of fibrous structures may be a critical first step in transmission.

Many studies on prion-like proteins in experimental models have suggested that sonication of amyloid or amyloid-like fibrils significantly enhances seeding activity. Fragmented amyloid fibrils induced cytotoxicity *in vitro* (33), and small soluble Aβ seeds found in brain extracts isolated from amyloid precursor protein transgenic mice caused intracerebral propagation *in vivo* (36). On the other hand, Wu *et al.* (32) reported that small tau aggregates were internalized in neuronal cells, and Jackson *et al.* (37) demonstrated that short fibrous tau assemblies with an average length of 179 nm isolated from P301S tau mice induced seed-dependent propagation *in vivo*. These findings are broadly consistent with our finding that fibrous α-syn seeds less than 50 nm in length (~40% of them were only 25 nm long) have the highest seeding activity in prion-like propagation. It is plausible that smaller structures would be more easily incorporated into cells by endocytosis. There is evidence that α-syn fibrous structures interact with cellular membranes, can move between cells, and are secreted from axons (38, 39). Additionally, Pieri *et al.* (40) reported that α-syn fibrils are more cytotoxic than oligomeric species. The presence of short fibrous structures in the supernatants after ultracentrifugation (41) or high-speed centrifugation (Fig. 4*B*) supports the possibility that oligomers (considered intermediates of fibrils) may include quite short fibrils. In prion proteins, nonfibrillar small particles showed the most infectivity, and sonication enhanced their transmissibility (42). Taking these results together, it seems that there are common features in the cell-to-cell spreading and transmission of pathogenic species of various prions and prion-like proteins.

In general, sonicated recombinant α-syn fibrils are used to induce cell-to-cell spreading in cellular and animal experimental models (23, 43), and it can be difficult to establish the relevance of such studies to the prion-like propagation seen in patients with α-synucleinopathies. However, the advantages of that approach are that well characterized short fibrils can be prepared and that inoculation samples are not contaminated with other factors that might influence propagation. However, there are clearly issues over interpretation because our data indicate that differences in preparation procedures, including the degree of sonication of preformed α-syn fibrils, can greatly influence the results. It is also noteworthy that familial PD α-syn mutant A30P fibrils are more fragile than WT α-syn fibrils (41).

In this work, we investigated the seeding activity of various α-syn species in various experimental models of prion-like propagation and found that fragmented β sheet-rich fibrous α-syn species (50 nm or less in length) were the most effective in inducing seed-dependent aggregation of α-syn in all experi-

mental models. Further study is needed to elucidate the precise mechanisms underlying the prion-like propagation.

## EXPERIMENTAL PROCEDUERS

*Expression, Purification, and Preparation of α-Syn Proteins*—Human wild-type α-syn and mouse wild-type α-syn in pRK172, a construct containing α-syn that lacks cysteine because of mutagenesis of codon 136 (TAC to TAT) as described previously (44), were transformed into *Escherichia coli* BL21 (DE3). Expression and purification were performed as described previously (45). The protein concentrations of α-syn were determined as described previously (45). Purified recombinant α-syn proteins (5 mg/ml) containing 30 mM Tris-HCl (pH 7.5), 10 mM DTT, and 0.1% sodium azide were incubated at 4 °C, room temperature (20~25 °C), and 37 °C with or without shaking. Incubation with shaking was done with a horizontal shaker (TAITEC) at 200 rpm. After incubation for 7 days, the samples were diluted to 2 mg/ml in saline. α-Syn samples were analyzed by 12% SDS-PAGE with 2-mercaptoethanol and stained with CBB. Immunoblotting with polyclonal antibody syn131–140 (1:2000) directed against a synthetic peptide (residues 131–140) (41, 46) was performed as described previously (47). Gel images were recorded with a Gel Doc™ EZ Imager (Bio-Rad).

*Electron Microscopy*—α-Syn samples were diluted in saline to 0.1 mg/ml, and 0.2-μg aliquots were dropped on carbon-coated 300-mesh copper grids (Nissin EM) and incubated for 3 min. After removal of surplus material, the samples were negatively stained for 3 min with a drop of 2% phosphotungstic acid and dried. Electron micrograph images were recorded with a JEM-1400 electron microscope (JEOL).

*Semiquantitative Analysis of the Length of Sonicated α-Syn Fibrils*—α-Syn fibrils were sonicated with an ultrasonic homogenizer (VP-5S, TAITEC) on ice for 0, 5, 15, 30, 60, and 180 s. Sonicated fibrils (0.1 mg/ml) were observed at a magnification of ×10,000 by electron microscopy. Fibril lengths were measured on photographs, and the length distribution was calculated.

*Thioflavin Fluorescence Assay*—The degree of fibrillation was measured in terms of ThS fluorescence intensity, which is increased upon binding to amyloid-like fibrils. The samples (10 μl) were incubated with 5 μM thioflavin S in 20 mM MOPS buffer (pH 6.8) for 30 min at room temperature. Fluorometry was performed using a microplate reader (440 nm excitation/521 nm emission) as described previously (48). For the α-syn seeding assay, amyloid-like fibril formation was monitored in terms of thioflavin T fluorescence (excitation 442 nm, emission 485 nm) with a plate reader (Varioskan™ Flash, Thermo Scientific). The reaction mixture included 100 μM α-syn monomer and 20 μM thioflavin T in 30 μM Tri-HCl (pH 7.4) in the absence or presence of 5 μM α-syn fibril seeds.

*Cell Culture, Transfection of Plasmids, and Introduction of α-Syn Proteins into Cells*—Human neuroblastoma SH-SY5Y cells were maintained at 37 °C in 5% $CO_2$ in DMEM/F12 medium (Sigma-Aldrich) supplemented with 10% fetal calf serum, penicillin-streptomycin glutamine (Gibco), and minimum Eagle's medium nonessential amino acid solution (Gibco). Cells were cultured to 40–50% confluence in collagen-coated 6-well plates and transfected using X-tremeGENE 9 (Roche Life Science) with pcDNA3 or pEGFP encoding wild-type human α-syn (1.5 μg) according to the instructions of the manufacturer. After transfection of plasmids, cells were incubated for 6–8 h, and α-syn samples (5 μg) were introduced using MultiFectam (Promega) according to the instructions of the manufacturer. Transfected cells were incubated for 2 days.

*Preparation of sarkosyl-insoluble Fractions of Cultured Cells and Immunoblotting*—Transfected SH-SY5Y cells were collected and extracted with 1 ml of 1% sarkosyl in A68 buffer (10 mM Tris-HCl (pH 7.5) containing 10% sucrose, 0.8 M NaCl, and 1 mM EGTA). Cell extracts were sonicated for 15 s on ice and collected as total cell lysates. After incubation for 30 min at 37 °C, cell extracts were ultracentrifuged at 113,000 × *g* for 20 min at 25 °C. The supernatants were removed and collected as sarkosyl-soluble fractions, and then the pellets were washed with 30 mM Tris-HCl (pH7.5) and ultracentrifuged as before. The resulting pellets were collected as sarkosyl-insoluble fractions, resuspended in 30 mM Tris-HCl (pH7.5), and sonicated for 15 s. Total cell lysates and sarkosyl-insoluble and -soluble fractions were added to SDS sample buffer and heated to 100 °C for 3 min. The protein concentrations of samples were determined by a Pierce BCA protein assay kit (Thermo Fisher Scientific). Total cell lysates and sarkosyl-insoluble and -soluble fractions were separated by 15% SDS-PAGE. Immunoblotting with mouse monoclonal antibody Ser(P)-129 (1:1000) directed against α-syn phosphorylated at Ser-129 (10) and polyclonal antibody syn131–140 (1:2000) was performed. Anti-Ser(P)-129 antibody was a kind gift from Dr. Takeshi Iwatsubo. Immunoblotting with monoclonal anti-α-tubulin (1:1000, Sigma) was used as a loading control. All experiments were performed at least three times. The band intensities of immunoblots were quantified using ImageJ software.

*Cell Viability Assay*—The cytotoxicity of SH-SY5Y cells was assessed by 3-(4,5-dimethylthiazol-2-yl)-2,5-diphenyltetrazolium bromide (MTT) assay using Cell Proliferation Kit I (Roche) according to the instructions of the manufacturer.

*Mice*—C57BL/6J mice were purchased from CLEA Japan, Inc. All experimental protocols were performed according to the Animal Care and Use Committee of the Tokyo Metropolitan Institute of Medical Science.

*α-Syn Inoculation into Mice and Immunohistochemistry*—α-Syn samples (10 μg) were injected into striatum (anterior-posterior, 0.2 mm; medial-lateral, −2.0 mm; dorsal-ventral, −2.6 mm). Inoculation into mouse brains was performed as described previously (19). 3 months after inoculation, mice were anesthetized with isoflurane and killed by decapitation. Brains were fixed with 10% formalin neutral buffer solution (Wako) and sectioned at 50 μm with a Leica VT1200S. Immunohistochemistry with polyclonal antibody 1175 (1:2000) directed against α-syn phosphorylated at Ser-129 was performed as described previously (19). For ThT staining, the sections were stained with 0.1% ThT in 80% ethanol for 15 min and then washed with 80% and 70% ethanol each for 1 min and distilled water twice. α-Syn pathologies were observed and recorded with a BZ-X710 (Keyence). α-Syn pathologies were quantified using a BZ-X analyzer (Keyence) and expressed as the percent area covered by phosphorylated α-syn deposits of

the total area. For preparation of sarkosyl-insoluble fractions, brains were snap-frozen on dry ice and stored at −80 °C.

*Preparation of sarkosyl-insoluble Fractions of Mouse Brains*—Frozen mouse brains were homogenized in 20 volumes (w/v) of A68 buffer and incubated for 30 min at 37 °C after addition of sarkosyl (final concentration, 2%). Brain homogenates were centrifuged at 9460 × *g* for 10 min at 25 °C, and then the supernatants were collected and ultracentrifuged at 113,000 × *g* for 20 min at 25 °C. The pellets were washed with saline and ultracentrifuged as before. The resulting pellets were collected as sarkosyl-insoluble fractions of mouse brains and resuspended in 30 mM Tris-HCl (pH 7.5).

*Immunoelectron Microscopy*—Sarkosyl-insoluble fractions extracted from injected mice were dropped onto carbon-coated nickel grids (Nissin EM). The grids were immunostained with primary antibodies (anti-mouse α-syn, syn 131–140, Ser(P)-129, 1:200) and secondary antibody conjugated to 10 nm gold particles (BBI Solutions, 1:50) as described previously (49). Polyclonal anti-mouse α-syn was obtained from Cell Signaling Technology. Electron micrograph images were recorded with a JEOL JEM-1400 electron microscope.

Pre-embedding immunoelectron microscopy of α-syn fibril-injected mice was performed as follows. Brains were fixed with 4% paraformaldehyde, 0.1% glutaraldehyde (GA) in phosphate buffer (pH 7.4) for 1 h and thinly sectioned. The sections were treated with 0.5% $H_20_2$ in methanol for 30 min and 0.05% Triton X-100 in PBS, blocked with 10% calf serum in PBS, and incubated with the primary antibody (1175, 1:200). After extensive washing, the sections were incubated with secondary antibody conjugated to nanogold particles (1:50). Immunostained sections were fixed with 2% glutaraldehyde in phosphate buffer at 4 °C overnight. The nanogold particles were enhanced with GOLDENHANCE EM Formulation (Nanoprobes), and the sections were dehydrated in graded ethanol solutions (50%, 70%, 90%, and 100%), infiltrated with propylene oxide, and polymerized in resin (Quetol-812, Nisshin EM) at 60 °C for 48 h. The polymerized resin were ultra-thin-sectioned at 80 nm using Ultracut UCT (Leica), and the sections were mounted on copper grids and stained for 15 min with 2% uranyl acetate. Electron micrograph images were recorded with a JEOL JEM-1400Plus electron microscope.

*Gel Filtration Chromatography*—α-Syn samples were centrifuged at 20,000 × *g* for 10 min at 25 °C. The supernatants and monomeric α-syn were analyzed by size-exclusion HPLC on a Superdex 200 Increase 5/150 GL (GE Life Sciences) equilibrated with 10 mM Tris-HCl (pH 7.5) and 0.15 M NaCl. Protein elution was monitored at 215 nm. Separated fractions were analyzed by 12% SDS-PAGE and stained with CBB.

*Live Cell Imaging*—α-Syn fibrils formed by shaking at 37 °C were labeled with an Alexa Fluor 546 protein labeling kit (Invitrogen) according to the instructions of the manufacturer. Fluorescence-labeled α-syn fibrils with or without sonication (180 s) were introduced into SH-SY5Y cells transfected with pEGFP wild-type human α-syn (1.5 μg) in 6-well plates. After introduction of α-syn fibrils, live-cell imaging was performed using a BZ-X710 (Keyence) with monitoring at multiple sample points every 15 min for 37 h. Cells were maintained at 37 °C and 5% $CO_2$ using an incubation system for microscopes (TOKAI HIT) during observation. Images were analyzed using a BZ-X analyzer (Keyence).

*Statistical Analysis*—Unpaired, two-tailed Student's test was used for all analyses in the figures. $p < 0.05$ was regarded as statistically significant.

*Author Contributions*—M. H. and A. T. designed the research and wrote the manuscript. A. T. performed most of the biochemical and immunofluorescence experiments. A. S. performed the immunohistochemistry analysis. H. A., T. N., and G. S. provided key reagents and conducted the experiments in cellular models. S. H., T. N., G. S., A. T., and M. H. analyzed the data.

**References**


1. Braak, H., Del Tredici, K., Rüb, U., de Vos, R. A., Jansen Steur, E. N., and Braak, E. (2003) Staging of brain pathology related to sporadic Parkinson's disease. *Neurobiol. Aging* **24,** 197–211
2. Kordower, J. H., Chu, Y., Hauser, R. A., Freeman, T. B., and Olanow, C. W. (2008) Lewy body-like pathology in long-term embryonic nigral transplants in Parkinson's disease. *Nat. Med.* **14,** 504–506
3. Li, J. Y., Englund, E., Holton, J. L., Soulet, D., Hagell, P., Lees, A. J., Lashley, T., Quinn, N. P., Rehncrona, S., Björklund, A., Widner, H., Revesz, T., Lindvall, O., and Brundin, P. (2008) Lewy bodies in grafted neurons in subjects with Parkinson's disease suggest host-to-graft disease propagation. *Nat. Med.* **14,** 501–503
4. Goedert, M. (2001) α-Synuclein and neurodegenerative diseases. *Nat. Rev. Neurosci.* **2,** 492–501
5. Maroteaux, L., Campanelli, J. T., and Scheller, R. H. (1988) Synuclein: a neuron-specific protein localized to the nucleus and presynaptic nerve terminal. *J. Neurosci.* **8,** 2804–2815
6. Burré, J., Sharma, M., Tsetsenis, T., Buchman, V., Etherton, M. R., and Südhof, T. C. (2010) α-Synuclein promotes SNARE-complex assembly *in vivo* and *in vitro*. *Science* **329,** 1663–1667
7. Chandra, S., Fornai, F., Kwon, H. B., Yazdani, U., Atasoy, D., Liu, X., Hammer, R. E., Battaglia, G., German, D. C., Castillo, P. E., and Südhof, T. C. (2004) Double-knockout mice for α- and β-synucleins: effect on synaptic functions. *Proc. Natl. Acad. Sci. U.S.A.* **101,** 14966–14971
8. Chandra, S., Gallardo, G., Fernández-Chacón, R., Schlüter, O. M., and Südhof, T. C. (2005) α-Synuclein cooperates with CSPα in preventing neurodegeneration. *Cell* **123,** 383–396
9. Baba, M., Nakajo, S., Tu, P. H., Tomita, T., Nakaya, K., Lee, V. M., Trojanowski, J. Q., and Iwatsubo, T. (1998) Aggregation of α-synuclein in Lewy bodies of sporadic Parkinson's disease and dementia with Lewy bodies. *Am. J. Pathol.* **152,** 879–884
10. Fujiwara, H., Hasegawa, M., Dohmae, N., Kawashima, A., Masliah, E., Goldberg, M. S., Shen, J., Takio, K., and Iwatsubo, T. (2002) α-Synuclein is phosphorylated in synucleinopathy lesions. *Nat. Cell Biol.* **4,** 160–164
11. Hasegawa, M., Fujiwara, H., Nonaka, T., Wakabayashi, K., Takahashi, H., Lee, V. M., Trojanowski, J. Q., Mann, D., and Iwatsubo, T. (2002) Phosphorylated α-synuclein is ubiquitinated in α-synucleinopathy lesions. *J. Biol. Chem.* **277,** 49071–49076
12. Spillantini, M. G., Schmidt, M. L., Lee, V. M., Trojanowski, J. Q., Jakes, R., and Goedert, M. (1997) α-Synuclein in Lewy bodies. *Nature* **388,** 839–840
13. Wakabayashi, K., Yoshimoto, M., Tsuji, S., and Takahashi, H. (1998) α-Synuclein immunoreactivity in glial cytoplasmic inclusions in multiple system atrophy. *Neurosci. Lett.* **249,** 180–182
14. Spillantini, M. G., Crowther, R. A., Jakes, R., Hasegawa, M., and Goedert, M. (1998) α-Synuclein in filamentous inclusions of Lewy bodies from Parkinson's disease and dementia with Lewy bodies. *Proc. Natl. Acad. Sci. U.S.A.* **95,** 6469–6473
15. Uversky, V. N., Li, J., and Fink, A. L. (2001) Evidence for a partially folded intermediate in α-synuclein fibril formation. *J. Biol. Chem.* **276,** 10737–10744
16. Crowther, R. A., Jakes, R., Spillantini, M. G., and Goedert, M. (1998) Syn-

thetic filaments assembled from C-terminally truncated α-synuclein. *FEBS Lett.* **436,** 309–312
17. Luk, K. C., Kehm, V., Carroll, J., Zhang, B., O'Brien, P., Trojanowski, J. Q., and Lee, V. M. (2012) Pathological α-synuclein transmission initiates Parkinson-like neurodegeneration in nontransgenic mice. *Science* **338,** 949–953
18. Luk, K. C., Song, C., O'Brien, P., Stieber, A., Branch, J. R., Brunden, K. R., Trojanowski, J. Q., and Lee, V. M. (2009) Exogenous α-synuclein fibrils seed the formation of Lewy body-like intracellular inclusions in cultured cells. *Proc. Natl. Acad. Sci. U.S.A.* **106,** 20051–20056
19. Masuda-Suzukake, M., Nonaka, T., Hosokawa, M., Oikawa, T., Arai, T., Akiyama, H., Mann, D. M., and Hasegawa, M. (2013) Prion-like spreading of pathological α-synuclein in brain. *Brain* **136,** 1128–1138
20. Nonaka, T., Watanabe, S. T., Iwatsubo, T., and Hasegawa, M. (2010) Seeded aggregation and toxicity of α-synuclein and tau: cellular models of neurodegenerative diseases. *J. Biol. Chem.* **285,** 34885–34898
21. Volpicelli-Daley, L. A., Luk, K. C., Patel, T. P., Tanik, S. A., Riddle, D. M., Stieber, A., Meaney, D. F., Trojanowski, J. Q., and Lee, V. M. (2011) Exogenous α-synuclein fibrils induce Lewy body pathology leading to synaptic dysfunction and neuron death. *Neuron* **72,** 57–71
22. Sacino, A. N., Thomas, M. A., Ceballos-Diaz, C., Cruz, P. E., Rosario, A. M., Lewis, J., Giasson, B. I., and Golde, T. E. (2013) Conformational templating of α-synuclein aggregates in neuronal-glial cultures. *Mol. Neurodegener.* **8,** 17
23. Luk, K. C., Kehm, V. M., Zhang, B., O'Brien, P., Trojanowski, J. Q., and Lee, V. M. (2012) Intracerebral inoculation of pathological α-synuclein initiates a rapidly progressive neurodegenerative α-synucleinopathy in mice. *J. Exp. Med.* **209,** 975–986
24. Masuda-Suzukake, M., Nonaka, T., Hosokawa, M., Kubo, M., Shimozawa, A., Akiyama, H., and Hasegawa, M. (2014) Pathological α-synuclein propagates through neural networks. *Acta Neuropathol. Commun.* **2,** 88
25. Recasens, A., Dehay, B., Bové, J., Carballo-Carbajal, I., Dovero, S., Pérez-Villalba, A., Fernagut, P. O., Blesa, J., Parent, A., Perier, C., Fariñas, I., Obeso, J. A., Bezard, E., and Vila, M. (2014) Lewy body extracts from Parkinson disease brains trigger α-synuclein pathology and neurodegeneration in mice and monkeys. *Ann. Neurol.* **75,** 351–362
26. Watts, J. C., Giles, K., Oehler, A., Middleton, L., Dexter, D. T., Gentleman, S. M., DeArmond, S. J., and Prusiner, S. B. (2013) Transmission of multiple system atrophy prions to transgenic mice. *Proc. Natl. Acad. Sci. U.S.A.* **110,** 19555–19560
27. Bousset, L., Pieri, L., Ruiz-Arlandis, G., Gath, J., Jensen, P. H., Habenstein, B., Madiona, K., Olieric, V., Böckmann, A., Meier, B. H., and Melki, R. (2013) Structural and functional characterization of two α-synuclein strains. *Nat. Commun.* **4,** 2575
28. Peelaerts, W., Bousset, L., Van der Perren, A., Moskalyuk, A., Pulizzi, R., Giugliano, M., Van den Haute, C., Melki, R., and Baekelandt, V. (2015) α-Synuclein strains cause distinct synucleinopathies after local and systemic administration. *Nature* **522,** 340–344
29. Chen, S. W., Drakulic, S., Deas, E., Ouberai, M., Aprile, F. A., Arranz, R., Ness, S., Roodveldt, C., Guilliams, T., De-Genst, E. J., Klenerman, D., Wood, N. W., Knowles, T. P., Alfonso, C., Rivas, G., *et al.* (2015) Structural characterization of toxic oligomers that are kinetically trapped during α-synuclein fibril formation. *Proc. Natl. Acad. Sci. U.S.A.* **112,** E1994–2003
30. Cremades, N., Cohen, S. I., Deas, E., Abramov, A. Y., Chen, A. Y., Orte, A., Sandal, M., Clarke, R. W., Dunne, P., Aprile, F. A., Bertoncini, C. W., Wood, N. W., Knowles, T. P., Dobson, C. M., and Klenerman, D. (2012) Direct observation of the interconversion of normal and toxic forms of α-synuclein. *Cell* **149,** 1048–1059
31. Winner, B., Jappelli, R., Maji, S. K., Desplats, P. A., Boyer, L., Aigner, S., Hetzer, C., Loher, T., Vilar, M., Campioni, S., Tzitzilonis, C., Soragni, A., Jessberger, S., Mira, H., Consiglio, A., *et al.* (2011) *In vivo* demonstration that α-synuclein oligomers are toxic. *Proc. Natl. Acad. Sci. U.S.A.* **108,** 4194–4199
32. Wu, J. W., Herman, M., Liu, L., Simoes, S., Acker, C. M., Figueroa, H., Steinberg, J. I., Margittai, M., Kayed, R., Zurzolo, C., Di Paolo, G., and Duff, K. E. (2013) Small misfolded Tau species are internalized via bulk endocytosis and anterogradely and retrogradely transported in neurons. *J. Biol. Chem.* **288,** 1856–1870
33. Xue, W. F., Hellewell, A. L., Gosal, W. S., Homans, S. W., Hewitt, E. W., and Radford, S. E. (2009) Fibril fragmentation enhances amyloid cytotoxicity. *J. Biol. Chem.* **284,** 34272–34282
34. Falcon, B., Cavallini, A., Angers, R., Glover, S., Murray, T. K., Barnham, L., Jackson, S., O'Neill, M. J., Isaacs, A. M., Hutton, M. L., Szekeres, P. G., Goedert, M., and Bose, S. (2015) Conformation determines the seeding potencies of native and recombinant Tau aggregates. *J. Biol. Chem.* **290,** 1049–1065
35. Aulić, S., Le, T. T., Moda, F., Abounit, S., Corvaglia, S., Casalis, L., Gustincich, S., Zurzolo, C., Tagliavini, F., and Legname, G. (2014) Defined α-synuclein prion-like molecular assemblies spreading in cell culture. *BMC Neurosci.* **15,** 69
36. Langer, F., Eisele, Y. S., Fritschi, S. K., Staufenbiel, M., Walker, L. C., and Jucker, M. (2011) Soluble Aβ seeds are potent inducers of cerebral β-amyloid deposition. *J. Neurosci.* **31,** 14488–14495
37. Jackson, S. J., Kerridge, C., Cooper, J., Cavallini, A., Falcon, B., Cella, C. V., Landi, A., Szekeres, P. G., Murray, T. K., Ahmed, Z., Goedert, M., Hutton, M., O'Neill, M. J., and Bose, S. (2016) Short fibrils constitute the major species of seed-competent Tau in the brains of mice transgenic for human P301S Tau. *J. Neurosci.* **36,** 762–772
38. Brahic, M., Bousset, L., Bieri, G., Melki, R., and Gitler, A. D. (2016) Axonal transport and secretion of fibrillar forms of α-synuclein, Aβ42 peptide and HTTExon 1. *Acta Neuropathol.* **131,** 539–548
39. Monsellier, E., Bousset, L., and Melki, R. (2016) α-Synuclein and huntingtin exon 1 amyloid fibrils bind laterally to the cellular membrane. *Sci. Rep.* **6,** 19180
40. Pieri, L., Madiona, K., Bousset, L., and Melki, R. (2012) Fibrillar α-synuclein and huntingtin exon 1 assemblies are toxic to the cells. *Biophys. J.* **102,** 2894–2905
41. Yonetani, M., Nonaka, T., Masuda, M., Inukai, Y., Oikawa, T., Hisanaga, S., and Hasegawa, M. (2009) Conversion of wild-type α-synuclein into mutant-type fibrils and its propagation in the presence of A30P mutant. *J. Biol. Chem.* **284,** 7940–7950
42. Silveira, J. R., Raymond, G. J., Hughson, A. G., Race, R. E., Sim, V. L., Hayes, S. F., and Caughey, B. (2005) The most infectious prion protein particles. *Nature* **437,** 257–261
43. Volpicelli-Daley, L. A., Luk, K. C., and Lee, V. M. (2014) Addition of exogenous α-synuclein preformed fibrils to primary neuronal cultures to seed recruitment of endogenous α-synuclein to Lewy body and Lewy neurite-like aggregates. *Nat. Protoc.* **9,** 2135–2146
44. Masuda, M., Dohmae, N., Nonaka, T., Oikawa, T., Hisanaga, S., Goedert, M., and Hasegawa, M. (2006) Cysteine misincorporation in bacterially expressed human α-synuclein. *FEBS Lett.* **580,** 1775–1779
45. Nonaka, T., Iwatsubo, T., and Hasegawa, M. (2005) Ubiquitination of α-synuclein. *Biochemistry* **44,** 361–368
46. Masuda, M., Hasegawa, M., Nonaka, T., Oikawa, T., Yonetani, M., Yamaguchi, Y., Kato, K., Hisanaga, S., and Goedert, M. (2009) Inhibition of α-synuclein fibril assembly by small molecules: analysis using epitope-specific antibodies. *FEBS Lett.* **583,** 787–791
47. Takahashi, M., Miyata, H., Kametani, F., Nonaka, T., Akiyama, H., Hisanaga, S., and Hasegawa, M. (2015) Extracellular association of APP and tau fibrils induces intracellular aggregate formation of tau. *Acta Neuropathol.* **129,** 895–907
48. Shimonaka, S., Nonaka, T., Suzuki, G., Hisanaga, S., and Hasegawa, M. (2016) Templated aggregation of TAR DNA-binding protein of 43 kDa (TDP-43) by seeding with TDP-43 peptide fibrils. *J. Biol. Chem.* **291,** 8896–8907
49. Hasegawa, M., Arai, T., Nonaka, T., Kametani, F., Yoshida, M., Hashizume, Y., Beach, T. G., Buratti, E., Baralle, F., Morita, M., Nakano, I., Oda, T., Tsuchiya, K., and Akiyama, H. (2008) Phosphorylated TDP-43 in frontotemporal lobar degeneration and amyotrophic lateral sclerosis. *Ann. Neurol.* **64,** 60–70